Eigenvalue Sensitivity Computations for Linear Stability Theory

Connor Klauss,[1] Pedro Paredes,[2] Meelan Choudhari,[3]
Boris Diskin,[2] & James Baeder[1]

[1]University of Maryland, College Park

[2]National Institute of Aerospace

[3]Computational AeroSciences Branch, NASA Langley Research Center

AIAA Aviation 2023
CFD-02: Boundary Layer Transition I
June 12-16, 2023, San Diego, CA, USA

Outline

How can we influence the transition onset location?

- Laminar-turbulent transition results in a large increase in skin-friction drag and overall heat loads
  - Several efforts to delay transition in boundary layer flows across speed regime
  - Optimization of transition control is critical to maximize the benefits of laminar flow technology
- Examples of optimization studies related to transition delay:
  - Optimal wall suction to suppress Tollmien-Schlichting (TS) and crossflow (CF) disturbances in boundary layers[1,2]
  - Adjoint-based optimization methods for airfoil shape design to optimize natural laminar flow (NLF) performance[3,4,5,6]

[1] J. Pralits and A. Hanifi. *Optimal suction design for HLFC applications*. AIAA Paper 2003-4164. 2003.

[2] C. Airiau et al. "A methodology for optimal laminar flow control: Application to the damping of Tollmien-Schlichting waves in a boundary layer". In: *Phys. Fluids* 15.5 (2006), pp. 1131–1145. DOI: 10.1063/1.1564605.

[3] Y. Shi et al. "Natural Laminar-Flow Airfoil Optimization Design Using a Discrete Adjoint Approach". In: *AIAA Journal* 58.11 (2020), pp. 4702–4722.

[4] O. Amoignon et al. "Shape Optimization for Delay of Laminar-Turbulent Transition". In: *AIAA Journal* 44.6 (2006), pp. 1009–1042.

[5] J.D. Lee and A. Jameson. *Natural-Laminar-Flow Airfoil and Wing Design by Adjoint Method and Automatic Transition Prediction*. AIAA Paper 2009-0897. 2009.

[6] D. Simanowitsch et al. *Comparison of Gradient-Based and Genetic Algorithms for Laminar Airfoil Shape Optimization*. AIAA 2022-0008. 2022.

How can we influence the transition onset location?

- In the supersonic/hypersonic regimes:
  - Ultrasonically absorptive surface coating[7]
  - Appropriately placed 2D roughness elements[8]
  - Suitable spanwise modulation of boundary layer flow via arrays of rougness elements[9,10,11]
- Optimization of transition-delay technologies can lead to substantial increases control effectiveness[12,13]
  - Use adjoint-based analysis to obtain sensitivity derivatives

[7] A. Fedorov et al. "Stabilization of a hypersonic boundary layer using an ultrasonically absrptive coating". In: *J. Fluid Mech.* 479 (2003), pp. 99–124.

[8] K.D. Fong et al. "Second mode suppression in hypersonic boundary layer by roughness: design and experiments". In: *AIAA J.* 53.10 (2015), pp. 3138–3143.

[9] P.F. Holloway and J.R. Sterrett. *Effect of controlled surface roughness on boundary-layer transition and heat transfer at Mach number of 4.8 and 6.0*. NASA TR-D-2054. 1964.

[10] P. Paredes, M.M. Choudhari, and F. Li. "Instability wave-streak interactions in a high Mach number boundary layer at flight conditions". In: *J. Fluid Mech.* 858 (2019), pp. 474–499.

[11] P. Paredes, M. Choudhari, and F. Li. *Transition delay via vortex generators in a hypersonic boundary layer at flight conditions*. AIAA Paper 2018-3217. 2018.

[12] C. Pederson et al. *Shape optimization of vortex generators to control Mack mode amplification*. AIAA Paper 2020-2963. 2020.

[13] C. Klauss et al. *Stability Analysis of Streaks Induced by Optimized Vortex Generators*. AIAA Paper 2018-1823. 2018.

Objectives

Long-Term Goal

- Integration of transition prediction based on linear stability analysis into adjoint-based design optimization
- Coupling of adjoint-enabled computational fluid dynamic (CFD) solver with an adjoint-enabled linear stability code

Present Study: Adjoint Linear Stability Solver

- Develop discrete adjoint formulation to directly determine the sensitivity of the transition location based on N-factor calculation with LST
- Verify adjoint formulation using a second-order central finite-difference (FD) approximation for sensitivity with respect to disturbance properties (frequency and spanwise wavenumber)
- Evaluate transition location sensitivity for subsonic, supersonic, and hypersonic boundary layers

Outline

Linear Stability Theory (LST)[14]

- Decomposition of flow variables:

$$\mathbf{q}(\xi,\eta,\zeta,t) = \bar{\mathbf{q}}(\xi,\eta,\zeta) + \tilde{\mathbf{q}}(\xi,\eta,\zeta,t)$$

- Definition of perturbations:

$$\tilde{\mathbf{q}}(\xi,\eta,\zeta,t) = \hat{\mathbf{q}}(\eta)\exp\left[\mathrm{i}\left(\alpha\xi + \beta\zeta - \omega t\right)\right]$$

- Generalized eigenvalue problem utilizing the companion matrix method:

$$\begin{aligned} \mathbf{A}\hat{\mathbf{q}}^{+} &= \alpha\mathbf{B}\hat{\mathbf{q}}^{+} \\ \hat{\mathbf{q}}^{+}(\eta) &= (\hat{\rho},\hat{u},\hat{v},\hat{w},\hat{T},\alpha\hat{u},\alpha\hat{v},\alpha\hat{w},\alpha\hat{T})^{T} \end{aligned}$$

- Transition onset estimated by using an N-factor criterion:

$$N(\xi) = \int_{\xi_0}^{\xi} \sigma(\xi')\,\mathrm{d}\xi';\ \sigma(\xi) = -\alpha_i(\xi);\ \sigma(\xi_0) = 0$$

- The N-factor envelope is calculated:

$$N_{env}(\xi,\beta) = \max_{\omega}(N(\xi,\omega,\beta))$$

[14] L.M. Mack. "Boundary layer linear stability theory". In: *AGARD–R–709. Special Course on Stability and Transition of Laminar Flow.* 1984, pp. 3.1–3.81.

Newton-Raphson Method for Generalized EVPs

- Reformulate discretized GEVP:
  - Remove one boundary condition: $\hat{v}_w = 0$
  - Apply an inhomogeneous boundary condition $\mathbf{e}_{\rho_\mathbf{w}}$

$$(\mathbf{A} - \alpha_{j-1}\mathbf{B})\hat{\mathbf{q}}_j = \mathbf{e}_{\rho_\mathbf{w}}$$

- Derive new system with respect to α:

$$(\mathbf{A} - \alpha_{j-1}\mathbf{B})\hat{\mathbf{q}}_{\alpha,j} = \mathbf{B}\hat{\mathbf{q}}_j, \quad \hat{\mathbf{q}}_{\alpha,j} \equiv \frac{\partial \hat{\mathbf{q}}_j}{\partial \alpha}$$

- Update eigenvalue until converged $\left(\hat{v}_{w,J} \approx 0 \text{ and } |\alpha_J - \alpha_{J-1}| < \epsilon\right)$:

$$\alpha_j = \alpha_{j-1} - \frac{\hat{v}_{w,j}}{\frac{\partial \hat{v}_{w,j}}{\partial \alpha}}, \quad \hat{v}_{w,j} = \mathbf{e}^T_{\hat{v}_w}, \ \frac{\partial \hat{v}_{w,j}}{\partial \alpha} = \mathbf{e}^T_{\hat{v}_w}\hat{\mathbf{q}}_{\alpha,j}$$

N-factor Envelope and Transition Location

- Finite number of frequencies to build envelope
- At each grid location ξ_i, discrete maximum may not be true maximum
  - Selection of frequencies
  - Calculation of N_{env}

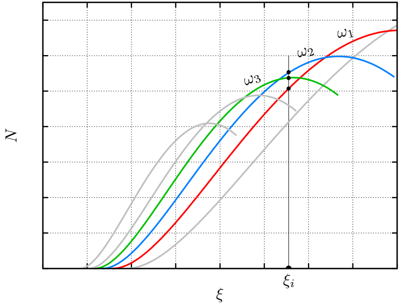

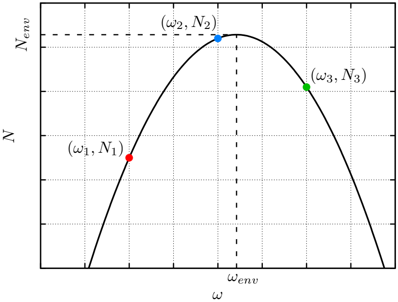

- At each ξ, sample data from three frequencies and construct parabola
- Differentiating the parabola yields the approximate value of N_{env} at that grid point
- Transition location is calculated with linear interpolation:

$$\xi_{tr} = \xi_L + \frac{N_{tr} - N_{env,\xi_L}}{N_{env,\xi_R} - N_{env,\xi_L}}(N_{env,\xi_R} - N_{env,\xi_L})$$

Formulation of Adjoint-Based Sensitivities

- Discrete adjoint formulation
- Transition location selected as objective function $J = \xi_{tr}$
- Lagrangian $\mathcal{L} = J + \lambda_{\xi_{tr}}^T [F(N_{env,\xi_L}, N_{env,\xi_R})] + ...$
  - N-factor envelope to the left/right of transition location: N_{env,ξ_L}, N_{env,ξ_R}
  - The N-factors from three frequencies composing N_{env}: $N_{\xi_L,k}$, $N_{\xi_R,k}$
  - The process for solving for the eigenvalue $\alpha_{j,i,k}$ and eigenvector $\hat{\mathbf{q}}_{j,i,k}$ at each ξ_i
- Taking the derivative of $\mathcal{L}$ with respect to a parameter of interest results in the sensitivity formulation

Outline

Results

Adjoint LST Eigenvalue Analysis

Verification

Incompressible ($M_e = 0.001$, $Re_0 = 400$)

- Adjoint LST eigenvalue verified using Blasius boundary layer
- Select $J = \sigma$ to calculate $\partial\sigma/\partial\omega$
- Differentiating $\mathcal{L}$ with respect to ω results in the sensitivity equation:

$$\frac{\partial\sigma}{\partial\omega} = \sum_{j=1}^{J}\left(\lambda_{\hat{\mathbf{q}}_j}^{T}\frac{\partial\mathbf{A}}{\partial\omega}\hat{\mathbf{q}}_j + \lambda_{\hat{\mathbf{q}}_{\alpha_j}}^{T}\frac{\partial\mathbf{A}}{\partial\omega}\hat{\mathbf{q}}_{\alpha_j}\right)$$

- Sensitivity is verified using a second-order central FD approximation

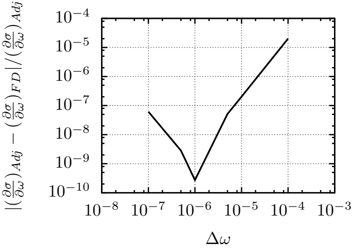

- FD approximation showed minimum error for $\Delta\omega = 10^{-6}$

Results

Adjoint Transition Prediction Analysis

Flat Plate Boundary Layer Flows

- Transition N-factor N_{tr} was chosen as 9.0 for each case in this study
- Leading instabilities for subsonic, supersonic, and hypersonic flows are Tollmien-Schlichting (TS), first mode (FM), and second mode (MM) waves, respectively
- Flow conditions of selected cases and respective dominant instability modes are shown in the following table ($Re_0 = 2000$)

Case	Mode	M_e	T_e (K)	$T_w/T_{w,ad}$
Subsonic	TS	0.85	219	1.0
Supersonic	FM	2.0	185	1.0
Hypersonic	MM	6.0	52.8	0.25

Verification

Incompressible ($M_e = 0.001$, $Re_0 = 400$)

- Adjoint transition prediction verified using Blasius boundary layer
- Select $J = \xi_{tr}$ to calculate $\partial \xi_{tr}/\partial \beta$
- Differentiating $\mathcal{L}$ with respect to β results in the sensitivity equation

$$\frac{\partial \xi_{tr}}{\partial \beta} = \sum_{k=1}^{3} \left\{ \sum_{i=0}^{n_{\xi_R}} \left[\sum_{j=1}^{J} \left(\lambda_{\hat{\mathbf{q}}_j}^T \left(\frac{\partial \mathbf{A}}{\partial \beta} - \alpha_{j-1} \frac{\partial \mathbf{B}}{\partial \beta} \right) \hat{\mathbf{q}}_j + \lambda_{\hat{\mathbf{q}}_{\alpha,j}}^T \left[\left(\frac{\partial \mathbf{A}}{\partial \beta} - \alpha_{j-1} \frac{\partial \mathbf{B}}{\partial \beta} \right) \hat{\mathbf{q}}_{\alpha,j} - \frac{\partial \mathbf{B}}{\partial \beta} \hat{\mathbf{q}}_j \right] \right) \right)_i \right\}_k$$

- Relative error

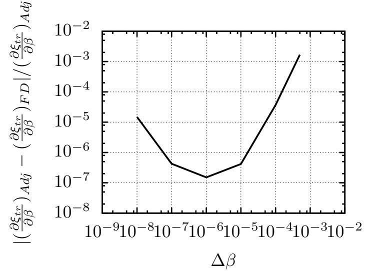

- Adjoint and FD sensitivities

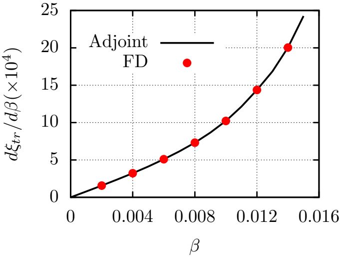

- FD showed best agreement with adjoint for $\Delta\beta = 10^{-6}$
- Adjoint and FD approximation results agree for range of β values

Sensitivity Derivatives

Subsonic ($M_e = 0.85$, $T_e = 219$ K, $Re_0 = 2000$)

- Leading instability: Planar TS waves

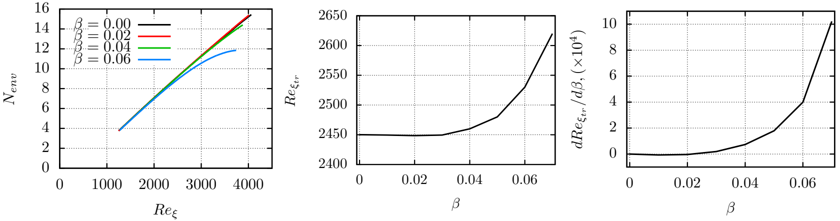

- As β increases, convexity is introduced to N_{env}
- This change in the shape of N_{env} pushes $Re_{\xi_{tr}}$ downstream
- The transition location proceeds slightly upstream and does not decrease until $\beta \approx 0.03$

Sensitivity Derivatives

Supersonic ($M_e = 2.0$, $T_e = 185$ K, $Re_0 = 2000$)

- Leading instability: Oblique FM waves

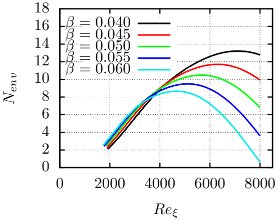

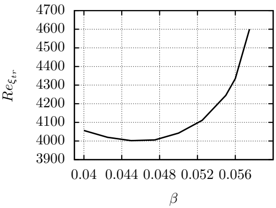

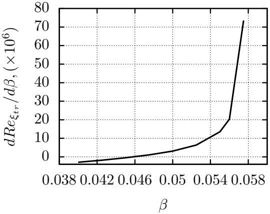

- As β increases, max(N_{env}) decreases, however the front pushes upstream
- With increasing β, the transition location first pushes upstream before retreating back downstream

Sensitivity Derivatives

Hypersonic ($M_e = 6.0$, $T_e = 52.8$ K, $Re_0 = 2000$)

- Leading instability: Planar MM waves

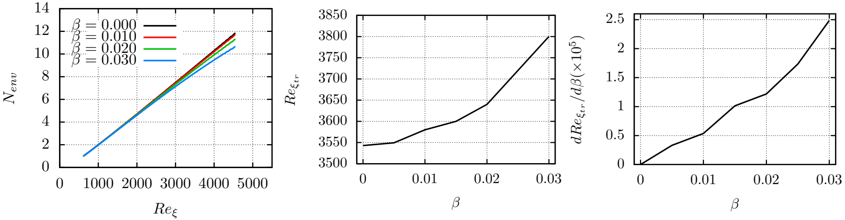

- As β increases, max(N_{env}) decreases slightly downstream
- With increasing β, the transition location pushes monotonically downstream

Secant Method Application

Supersonic ($M_e = 2.0$, $Re_0 = 2000$)

- Goal is to efficiently drive the derivative $\partial Re_{\xi_{tr}}/\partial\beta$ to zero, giving us the leading spanwise wavenumber for transition location, β_{tr}
- For this problem, the iterative secant method takes the form:

$$\beta_{i+1} = \beta_i - \left(\frac{\partial \xi_{tr}}{\partial \beta}\right)_i \frac{\beta_i - \beta_{i-1}}{\left(\frac{\partial \xi_{tr}}{\partial \beta}\right)_i - \left(\frac{\partial \xi_{tr}}{\partial \beta}\right)_{i-1}}$$

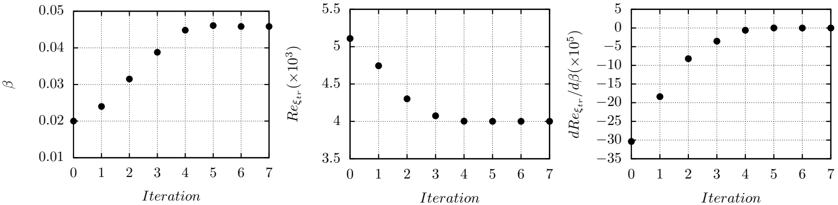

- After five iterations, the derivative is pushed to a relative zero
- The secant method quickly approches β_{tr}
- The transition front is pushed to its most upstream location

Outline

Summary and Conclusions

- The formulation for an adjoint-based sensitivity analysis of the transition location is presented.
- The sensitivity of the transition location with respect to spanwise wavenumber is investigated for subsonic, supersonic, and hypersonic flow regimes.
- The formulation has been shown to efficiently identify leading unstable spanwise wavenumbers in the supersonic regime.
- Future work will involve expanding the adjoint's capabilities by coupling with the FUN3D solver to allow for shape optimization in pursuit of transition delay.

Acknowledgments

- This material is based upon work supported by
  - the Air Force Office of Scientific Research under award number FA9550-20-0023 with P.O. Dr. Sarah Popkin
  - the NASA Hypersonic Technology Project (HTP) under the Aeronautics Research Mission Directorate (ARMD)
  - the NASA Transformational Tools and Technologies (TTT) project of the Transformative Aeronautics Concepts Program (TACP) under the ARMD
- Resources supporting this work are provided by
  - Department of Defense (DOD) High Performance Computing Modernization Program (HPCMP)
  - NASA High-End Computing (HEC) Program through the NASA Advanced Supercomputing (NAS) Division at Ames Research Center
  - NASA K-cluster at the Langley Research Center